Sugar Coating of Boron Powder for Efficient Carbon Doping of MgB2 with Enhanced Current-Carrying Performance

ARTICLE *in* ADVANCED MATERIALS · APRIL 2007

Impact Factor: 17.49 · DOI: 10.1002/adma.200601659

4 AUTHORS:

Shiguo Zhou
University of Wisconsin–Madison
69 PUBLICATIONS **8,017** CITATIONS
SEE PROFILE

Alexey V Pan
University of Wollongong
119 PUBLICATIONS **1,303** CITATIONS
SEE PROFILE

David Wexler
University of Wollongong
174 PUBLICATIONS **4,887** CITATIONS
SEE PROFILE

S. X. Dou
University of Wollongong
1,424 PUBLICATIONS **20,155** CITATIONS
SEE PROFILE

DOI: 10.1002/adma.200601659

Sugar Coating of Boron Powder for Efficient Carbon Doping of MgB_2 with Enhanced Current-Carrying Performance**

By *Sihai Zhou*, *Alexey V. Pan*,* *David Wexler*, and *Shi X. Dou*

The second boom in superconductivity during the last two decades has been powered up by the discovery of MgB_2 having the transition temperature (T_c) of 39 K[1] as well as a strong market potential for applications. The strongest impact on the development of this superconductor has been made by the discovery of the significant enhancement of the critical current density (J_c) as a function of the applied magnetic field (B_a) that results from SiC nanodoping.[2] Since then, a large variety of dopants have been attempted in order to achieve or improve on the attained enhancement.[3–11] In the vast majority of these doping works the nanodopants have been introduced via a solid-state reaction;[12–17] however, an important challenge is achieving homogeneity between a small amount of nanoadditives and matrix materials, because any dry mixing poses the major problem of nanoparticle agglomeration. In this Communication, we have chosen sugar ($C_6H_{12}O_6$) as the dopant. This is the most readily available carbohydrate that enables liquid homogeneous mixing. We have demonstrated that sugar doping resulted in an effective substitution of carbon for boron in MgB_2, so that a significant enhancement of the J_c performance over the entire applied field range is readily achievable. This method is applicable to the fabrication of a wide range of carbon-based compounds and composites.

The MgB_2 superconductor has a strong potential for various applications because of its high T_c, strong connectivity between the grains, and low anisotropy.[18] One major problem is posed by the relatively weak pinning in the pure material, which leads to rather rapid degradation of J_c as a function of B_a. Different approaches, such as irradiation and chemical doping, have been used to enhance the pinning strength in MgB_2.[2,4–6,10,11,17,19]. Chemical doping is a desirable, relatively easy, and cheap method to introduce pinning sites into the superconductor. Nanometer-size SiC has been found to be the most effective dopant for J_c enhancement.[2,5,6,15,20–22] The carbon-based materials introduce the strongest enhancement of $J_c(B_a)$ performance in MgB_2, owing to the fact that carbon can be incorporated into the MgB_2 crystal lattice by replacing boron. This substitution results in the enhancement of charge-carrier scattering occurring on C-substituted sites and Mg-vacancies in two energy bands discovered in this material.[23] This scattering has been shown to be responsible for the considerable upper critical field increase.[24] Generally, nanometer-sized particles are necessary to ensure a homogeneous doping procedure, which in our case should provide a strong enhancement of the pinning force. However, regardless of how well mixing, grinding,[2,5] milling, or ultrasonic dispersion[16] is carried out, the doping process is usually impeded by the formation of large agglomerates of particles. In addition, the precursor materials are commonly in their passivated state, which can further degrade the reactivity and doping quality.[25,26] Another problem for sustainable industrial applications is that nanometer-sized powders are expensive. Herein, we introduce a new approach to simple molecular mixing that ensures i) homogeneity, ii) strong reactivity with a maximum reaction surface, iii) fresh and clean interfaces between the atomic-scale dopant layer (C) and matrix components (B and Mg), and iv) rules out the necessity of nanometer-scale additives. This is achieved by "wet" mixing of a sugar solution with a boron powder and successive drying of the slurry to achieve homogeneous doping, resulting in $J_c(B_a)$ enhancements comparable to the best results achieved by SiC nanoscale doping.

Scanning electron microscopy (SEM) images of the raw and the sugar-coated boron powders show no difference. Both powders have ball-shaped particles down to a few nanometers in size. In contrast with pure MgB_2 formation upon heat treatment, the sugar-added powder first undergoes the decomposition of sugar to, most likely, water and fresh highly reactive carbon above 100 °C: $C_6H_{12}O_6 \rightarrow 6H_2O + 6C$. Concurrently, the following process may also occur: $C_6H_{12}O_6 \rightarrow 6CO + 6H_2$. However, the first route is more likely to occur, as can be concluded from the obtained X-ray diffraction (XRD) results. XRD pattern analysis of the MgB_2 samples indicates that the sugar slightly affects the phase constituents. Figure 1a shows XRD patterns of wet premixed MgB_2 samples with different levels of $C_6H_{12}O_6$ content. The samples mainly consist of an MgB_2 phase, with some MgO phase as the main impurity even for the sample with no sugar addition (carbon substitution level (x) equal to 0). This is probably a remnant effect of hydrotreatment and/or the presence of water in the sugar. Starting from 5 % sugar addition ($x = 0.08$), the $C_6H_{12}O_6$-doped samples show two peaks that belong to Mg_2C_3. For the $x = 0.03$ doping level sample only one small Mg_2C_3 peak is observed, as a result of the low amount of sugar added. Surprisingly, the

[*] Dr. A. V. Pan, Dr. S. Zhou, Dr. D. Wexler, Prof. S. X. Dou
Institute for Superconducting and Electronic Materials
University of Wollongong
Northfields Avenue, Wollongong, NSW 2522 (Australia)
E-mail: pan@uow.edu.au

[**] The authors thank O. Shcherbakova, X. Wang, and T. Silver for fruitful discussions. This project was financially supported by the Australian Research Council.

ADVANCED MATERIALS

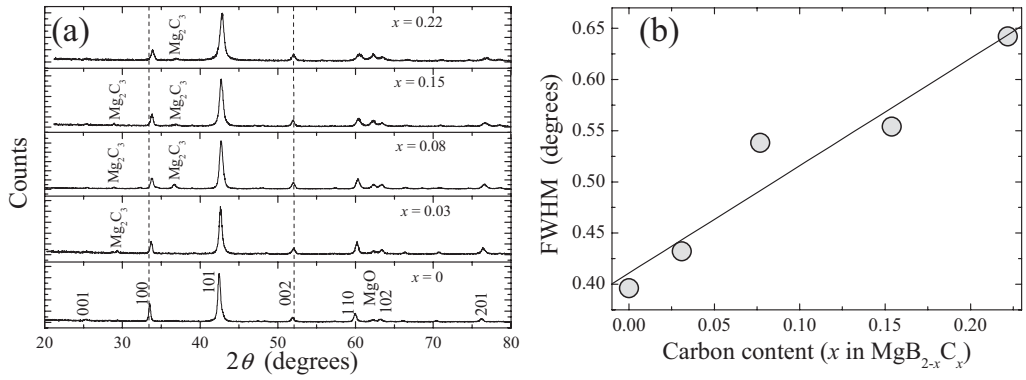

Figure 1. a) XRD patterns of $MgB_{2-x}C_x$ doped with different levels of sugar. The dotted lines indicate the positions of (100) and (002) peaks of pure MgB_2. b) The FWHM of the (101) peak as a function of the carbon content.

Mg_2C_3 peaks almost disappear in the sample with 15 % sugar added ($x = 0.22$). This can be explained by the competition between C, B, O, and H_2O to react with Mg. As the amount of the added sugar increases, the amounts of oxygen (and water) increase as well. Hence, Mg still predominantly reacts with B to form MgB_2 and increasingly with O (H_2O) to form MgO, as can be seen from the increasing MgO peak at $2\theta = 62.3°$, but instead ever less with C, as can be seen from the gradually vanishing Mg_2C_3 peaks. The dashed lines in Figure 1 show the position of the (100) and (002) peaks of a pure MgB_2 sample. Even at the small scale exhibited, it is obvious that the position of the (100) peak shifts to larger 2θ angles with increased levels of added $C_6H_{12}O_6$. This shift indicates a contraction of the *a*-axis of the crystal lattice.[5] In Figure 2, the change of the lattice parameter (Δa) is shown as a function of x in $MgB_{2-x}C_x$. The decrease of this parameter is an indication of the level of carbon-for-boron substitution.[13] The *a*-axis decreases linearly with increasing doping level, which implies that the solubility limit of C in MgB_2 has not been reached.[14] The position of the (002) peak shows no obvious shift with an increasing level of sugar doping; therefore, the change of the *c*-axis is negligible for the doping levels investigated.

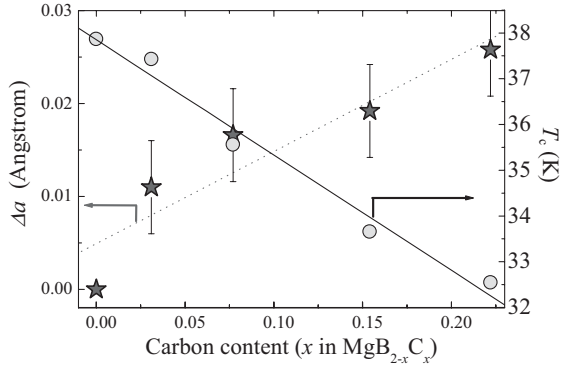

Figure 2. Critical temperature onset (circles) and the *a*-parameter of the crystal lattice as function of the carbon content of MgB_2 samples with added sugar (stars). The lines are linear fits to the data.

Another feature of the XRD patterns is the broadening of the peaks for the $C_6H_{12}O_6$-doped samples. Figure 1b shows the full width at half maximum (FWHM) value of the (101) peak of the different samples, which also shows a linear increase with increasing x in a similar manner as for SiC-doping.[27] This increase can imply a systematic structural change in the MgB_2 microstructure with increasing doping level. The increase of the FWHM value is a strong indication of a systematic reduction in grain size, as can be seen from a comparison between TEM images of pure MgB_2 and sugar-doped MgB_2 (Fig. 3). The reduction in grain size is probably a result of impurity particles introduced by the doping, which serve as additional nucleation sites for grain formation. The additional impurity particles and, thus, nucleation sites can restrict the mobility of grain walls, preventing them from growth.

The transition temperature onset (T_c) for the doped and undoped samples was determined by ac susceptibility measurements (Fig. 2). As can be seen, the T_c decreases with increasing x. The reduction is similar to that of C doping[17] but is larger than that of SiC-doped samples.[2,5]

The $J_c(B_a)$ curves, recorded at 5 and 20 K, for samples doped with different levels of sugar are shown in Figure 4. In general, the sugar-doped MgB_2 samples show a drastic enhancement of J_c compared with pure MgB_2. The level of enhancement in high magnetic fields for the samples with $x = 0.08$ to 0.15 is very similar to the level of J_c increase exhibited by SiC doping.[2,5,6] As can be seen, the water formed after the decomposition of sugar does not pose a substantial threat to the final electromagnetic properties. This may be due to the fact that the presence of a small amount of MgO before the formation of MgB_2 has a negligible effect on the final properties of the MgB_2 superconductor.[25] However, an even more interesting and significant result is that obtained for the relatively small level of doping, $x = 0.03$: at small fields $J_c(B_a)$ does not undergo any notable degradation. This is in contrast with results obtained from SiC doping and other, similar C-containing dopants.[2,5,6,13,16,28] For larger values of x, the trend in the $J_c(B_a)$ behavior becomes quite similar to the SiC-

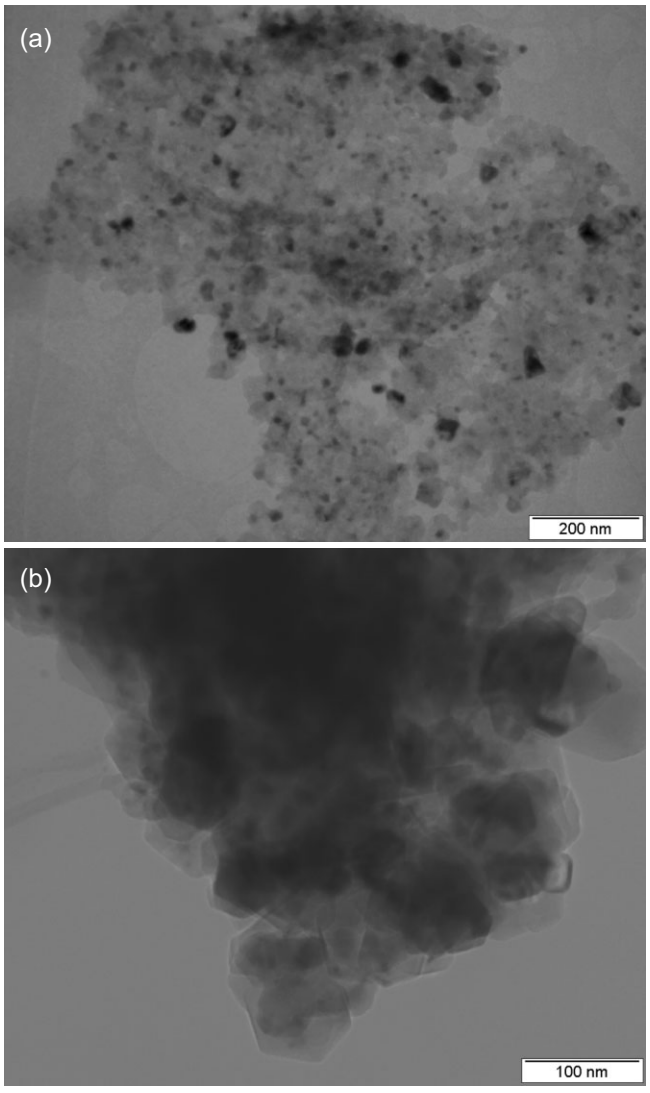

Figure 3. TEM images for a) a sample doped with 10% sugar ($x = 0.15$), and b) a pure MgB_2 sample.

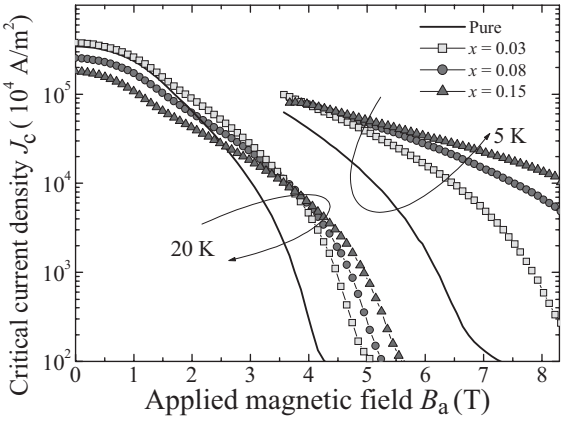

Figure 4. $J_c(B_a)$ curves for MgB_2 samples doped with different levels of sugar.

doping: the J_c degradation in low fields is a result of reduced transparency (stronger charge-carrier scattering) for the current flow, and the strong enhancement in high fields is a result of stronger flux pinning on additional defects produced by the C substitution and nanoscale inclusions such as MgO and Mg_2C_3.[15,23] Whereas the sample with $x = 0.15$ has reached the enhancement level of the optimal SiC-doping, the MgB_2 sample shows slightly smaller J_c values than optimally prepared pure MgB_2.[13] The observed degradation for the pure "reference" sample may be caused by a remnant effect from the water mixing and, subsequently, more considerable MgO formation (Fig. 1a).

The TEM images show that the impurities in the sugar-doped sample are homogeneously distributed within the MgB_2 matrix (Fig. 3a). The doped sample contains impurity particles. The size of the particles varies from 10 to 50 nm, which is slightly larger than after SiC doping (5 to 30 nm).[2,5] The selected area electron diffraction (SAED) patterns exhibit MgB_2 and MgO rings for both samples (data not shown). There is also a weak Mg_2C_3 ring in the doped sample. Energy dispersive X-ray spectroscopy (EDX) has been used to detect the elemental distribution. Higher oxygen levels are found in the doped sample compared with the undoped sample. In some locations boron-rich areas can be found, indicating excess boron as a result of the reaction between magnesium and oxygen/carbon.

In summary, doping with carbohydrates, such as sugar, provides an efficient and desirable way of homogeneous, inexpensive, and degradation-free mixing with host precursor materials. This approach results in atomic-scale coating of each boron particle with sugar and enables efficient homogeneous doping, in contrast with the conventional sophisticated mixing of powders, even with nanometer-sized particles. The application of this method to MgB_2 leads to an enhancement of in-field J_c values by more than an order of magnitude; the same excellent results as the best developed route for nanoscale SiC-powder doping. Moreover, this approach provides an additional benefit to the $J_c(B_a)$ performance at low fields, that is, at low fields J_c does not degrade for certain doping levels as it does for any other C-doping method. This indicates that effective substitution of carbon for boron occurs without precipitation of the dopant or byproduct, such as MgO, at the grain boundaries, and hence the connectivity between grains is not affected, so that the transparency for the supercurrent flow remains as high as for the pure samples. To further reduce the effect of the presence of water and its influence on the electromagnetic properties, we are currently exploring the "wet" mixing procedure of hydrocarbons in nonaqueous solvents.

This finding opens up a new direction for manufacturing nanometer-scale added materials using a solution route rather than solid nanometer-scale additives. This not only solves the agglomeration problem and avoids the use of expensive nanometer-scale materials, but also achieves atomic-level mixing and strongly improved performance properties.

ADVANCED MATERIALS

Experimental

Polycrystalline MgB_2 samples doped with different level of sugar were prepared through an in situ reaction process. High-purity powders of magnesium (99 %), amorphous boron (99 %), and commercial white sugar were weighed out according to a MgB_2:$C_6H_{12}O_6$ weight ratio so that 0 %, 2 %, 5 %, 10 %, and 15 % of sugar was added to MgB_2; these additions corresponded, respectively, to C substitution for B in the $MgB_{2-x}C_x$ compound with the following x levels: $x = 0$, 0.03, 0.08, 0.15, and 0.22. The boron and $C_6H_{12}O_6$ powders were first mixed with the mortar and pestle by hand. Distilled water was used to help the mixing during the grinding. The slurry of the boron and sugar mixture was dried in a vacuum chamber at a slightly elevated temperature to remove water contained in the sugar. To enable comparison between doped and pure samples, boron powder without sugar was also mixed with water and dried in the vacuum chamber. After drying, the powders were ground, mixed with Mg powder, and ground again. The as-obtained powders, with and without sugar, were put into a pressure die with an inner diameter of 13 mm and pressed into pellets at a pressure of 8 MPa. The precursor pellets were sealed inside iron tubes, and sintered at 780 °C for 1 h in flowing argon gas until the furnace cooled down to room temperature. The phase and crystal structure of all the samples were analyzed by XRD with a Phillips diffractometer employing Cu Kα radiation. Grains of the powders and microstructures of the samples were observed by scanning electron microscopy (SEM). Transition electron microscopy (TEM) was employed to investigate the nanostructure of the samples. The magnetization curves were measured over a temperature range of 5 to 30 K by using a Physical Property Measurement System (PPMS, Quantum Design) in a time varying applied magnetic field with a sweep rate of 50 Oe s^{-1} (1 Oe = $10^3/(4\pi)$ A m^{-1}) over the range of $|B_a| \leq 8.5$ T. Rectangular samples with dimensions of $1 \times 2 \times 3$ mm, were cut from each pellet and polished before measurements. The field was applied along the longest sample dimension. The magnetic J_c was calculated from the height of the magnetization loop M by using the critical state model: $J_c = 12\ M\,b/d(3b - d)$, where b and d are the dimensions of the samples perpendicular to the direction of applied magnetic field and $d < b$. The $J_c(B_a)$ dependence at small fields and 5 K could not be measured because of thermomagnetic flux jumps. T_c was determined at the onset of the diamagnetism by measuring the real part of the ac susceptibility with the ac magnetic field amplitude of 0.1 Oe at a frequency of 117 Hz.

Received: July 23, 2006
Revised: September 25, 2006
Published online: April 19, 2006

[1] J. Nagamatsu, N. Nakagawa, T. Muranaka, Y. Zenitani, J. Akimitsu, *Nature* **2001**, *410*, 63.
[2] S. X. Dou, A. V. Pan, S. Zhou, M. Ionescu, H. K. Liu, P. R. Munroe, *Supercond. Sci. Technol.* **2002**, *15*, 1587.
[3] H. Kumakura, H. Kitaguchi, A. Matsumoto, H. Hatakeyama, *Appl. Phys. Lett.* **2004**, *84*, 3669.
[4] B. J. Senkowicz, J. E. Giencke, S. Patnaik, C. B. Eom, E. E. Hellstrom, D. C. Larbalestier, *Appl. Phys. Lett.* **2005**, *86*, 202 502.
[5] S. X. Dou, A. V. Pan, S. Zhou, M. Ionescu, X. L. Wang, J. Horvat, H. K. Liu, P. R. Munroe, *J. Appl. Phys.* **2003**, *94*, 1850.
[6] S. X. Dou, S. Soltanian, J. Horvat, X. L. Wang, P. Munroe, S. H. Zhou, M. Ionescu, H. K. Liu, M. Tomsic, *Appl. Phys. Lett.* **2002**, *81*, 3419.
[7] S. Soltanian, J. Horvat, X. L. Wang, P. Munroe, S. X. Dou, *Phys. C* **2003**, *390*, 185.
[8] R. H. T. Wilke, S. L. Bud'ko, P. C. Canfield, D. K. Finnemore, R. J. Suplinskas, S. T. Hannahs, *Phys. Rev. Lett.* **2004**, *92*, 217 003.
[9] V. Braccini, A. Gurevich, J. E. Giencke, M. C. Jewell, C. B. Eom, D. C. Larbalestier, A. Pogrebnyakov, Y. Cui, B. T. Liu, Y. F. Hu, J. M. Redwing, Q. Li, X. X. Xi, R. K. Singh, R. Gandikota, J. Kim, B. Wilkens, N. Newman, J. Rowell, B. Moeckly, V. Ferrando, C. Tarantini, D. Marré, M. Putti, C. Ferdeghini, R. Vaglio, E. Haanappel, *Phys. Rev. B* **2004**, *71*, 012 504.
[10] Y. Ma, X. Zhang, G. Nishijima, K. Watanabe, S. Awaji, X. Bai, *Appl. Phys. Lett.* **2006**, *88*, 072 502.
[11] A. Yamamoto, J. I. Shimoyama, S. Ueda, I. Iwayama, S. Horii, K. Kishio, *Supercond. Sci. Technol.* **2005**, *18*, 1323.
[12] S. X. Dou, W. K. Yeoh, O. Shcherbakova, D. Wexler, Y. Li, Z. M. Ren, P. Munroe, S. K. Tan, B. A. Glowacki, J. L. MacManus-Driscoll, *Adv. Mater.* **2006**, *18*, 785.
[13] S. X. Dou, W. K. Yeoh, J. Horvat, M. Ionescu, *Appl. Phys. Lett.* **2003**, *83*, 4996.
[14] M. Avdeev, J. D. Jorgensen, R. A. Ribeiro, S. L. Bud'ko, P. C. Canfield, *Phys. C* **2003**, *387*, 301.
[15] O. Shcherbakova, A. V. Pan, S. Soltanian, S. X. Dou, D. Wexler, *IEEE Trans. Appl. Supercond.* **2007**, in press.
[16] W. K. Yeoh, J. H. Kim, J. Horvat, S. X. Dou, P. Munroe, *Supercond. Sci. Technol.* **2006**, *19*, L5.
[17] T. Masui, S. Lee, A. Yamamoto, H. Uchiyama, S. Tajima, *Phys. C* **2004**, *412*, 303.
[18] D. C. Larbalestier, L. D. Cooley, M. O. Rikel, A. A. Polyanskii, J. Jiang, S. Patnaik, X. Y. Cai, D. M. Feldmann, A. Gurevich, A. A. Squitieri, M. T. Naus, C. B. Eom, E. E. Hellstrom, R. J. Cava, K. A. Regan, *Nature* **2001**, *410*, 186.
[19] Y. Bugoslavsky, L. F. Cohen, G. K. Perkins, M. Polichetti, T. J. Tate, R. Gwilliam, A. D. Caplin, *Nature* **2001**, *411*, 561.
[20] T. Nakane, C. H. Jiang, T. Mochiku, H. Fujii, T. Kuroda, H. Kumakura, *Supercond. Sci. Technol.* **2005**, *18*, 1337.
[21] S. X. Dou, V. Braccini, S. Soltanian, R. Klie, Y. Zhu, S. Li, X. L. Wang, D. Larbalestier, *J. Appl. Phys.* **2004**, *96*, 7549.
[22] M. D. Sumption, M. Bhatia, M. Rindfleisch, M. Tomsic, S. Soltanian, S. X. Dou, E. W. Collings, *Appl. Phys. Lett.* **2005**, *86*, 092 507.
[23] I. I. Mazin, O. K. Andersen, O. Jepsen, O. V. Dolgov, J. Kortus, A. A. Golubov, A. B. Kuz'menko, D. van der Marel, *Phys. Rev. Lett.* **2002**, *89*, 107 002.
[24] A. Gurevich, *Phys. Rev. B* **2003**, *67*, 184 515.
[25] S. Zhou, A. V. Pan, J. Horvat, M. Qin, H. K. Liu, *Supercond. Sci. Technol.* **2004**, *17*, S528.
[26] S. K. Chen, K. A. Yates, M. G. Blamire, J. L. MacManus-Driscoll, *Supercond. Sci. Technol.* **2005**, *18*, 1473.
[27] O. V. Shcherbakova, A. V. Pan, S. X. Dou, unpublished.
[28] C. H. Cheng, H. Zhang, Y. Zhao, Y. Feng, X. F. Rui, P. Munroe, H. M. Zeng, N. Koshizuka, M. Murakami, *Supercond. Sci. Technol.* **2003**, *16*, 1182.

